the same size and geometry, show comparable formation constants. These two alcohols must be too large compared to the β-CD cavity and hence give smaller formation constants compared to cyclopentanol. Benzyl alcohol, still larger, shows an even smaller formation constant. In contrast, 2-propanol is of smaller size than the open end of the β-CD cavity and also gives rise to less interaction than in the case of cyclopentanol.

Conclusions

Our data clearly demonstrate that proper size matching between the β-CD/pyrene complex and the alcohol strongly affects the stability of the ternary complex. Alcohols too small or too large compared to the open end of the β-CD cavity give formation constants that are smaller than those with the proper size such as *n*-butanol and cyclopentanol. Two of the most probable configurations for the β-CD/pyrene/cyclopentanol complex are shown below (not drawn to scale), with the hydrophobic part of the

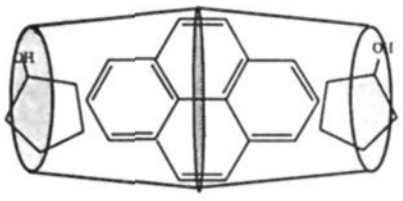

Type I

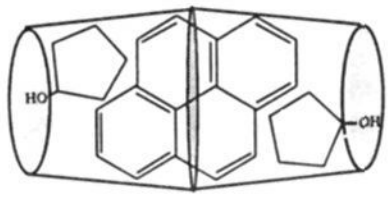

Type II

alcohol extending inside the cavity. For type I configuration, the pyrene is oriented axially inside the cavity with the alcohol capping the open end of each β-CD. In type II configuration, pyrene is positioned at an angle inside the two CDs. This allows for a stronger interaction between the alcohol and the protons located on the interior of the β-CD torus. The 2:1:2 β-CD/pyrene/alcohol stoichiometry suggests that the alcohol is on the primary side of the β-CD molecule. It should be noted that the orientation for the pyrene and alcohol in our depiction of the type II interaction is somewhat arbitrary and is not meant to depict the exact configuration of the complex.

From the mixed-alcohol results, it is evident that 2-methyl-2-propanol displaces ethanol, *n*-propanol, *n*-butanol, or 2-propanol from the complex, independent of the I/III ratios obtained for the different ternary complexes formed. This observation strongly supports the role of the size and volume of the alcohol and is in agreement with the trend found in the values for the formation constant. Other experiments performed with different mixtures are also consistent with these observations.

Acknowledgment. This work was supported in part by the National Science Foundation (CHE-9001412) and the National Institutes of Health (GM 39844). We thank the NSF (CHE-8206103) for the use of an NT-360 NB as a shared instrument. A.M.P. acknowledges support from DGICYT of the Ministry of Education and Science of Spain for the grant that made possible his research in Professor Warner's laboratory. We are grateful to Dr. L. G. Marzilli for useful discussions regarding the NMR data and G. A. Reed of American Maize Products for providing CDs used in this study.

Diimide Formation on Rhodium Surfaces: A Temperature-Programmed Reaction Spectroscopy Study

Jagdish Prasad and John L. Gland*

Contribution from the Department of Chemistry, The University of Michigan, Ann Arbor, Michigan 48109-1055. *Received January 29, 1990. Revised Manuscript Received August 9, 1990*

Abstract: Diimide (N_2H_2) formation has been detected as a gas-phase product over the 180–500 K temperature range from a clean rhodium surface during decomposition of both hydrazine and ammonia. The diimide was identified on the basis of mass spectrometry of the parent ion (30 amu) and a single-dehydrogenation fragmentation product (29 amu) that is 6% of the parent. The formation of diimide was confirmed chemically for both precursors by observing substantial increases in yield in the presence of coadsorbed hydrogen and a substantial decrease in the presence of coadsorbed oxygen. Adsorbed NH from N_2H_4 or NH_3 decomposition is proposed as a potential surface intermediate.

Diimide (N_2H_2), the parent of azo compounds, is of great interest to chemists because of its important role as an active reducing agent in synthetic chemistry[1-4] and as a transient intermediate in a variety of gas-phase reactions.[2] Previous studies relating to diimide formation and characterization have been in solution, or low-temperature matrices where the diimide was formed in microwave discharges.[5-8] We report in this paper, to the best of our knowledge, the first observation of diimide formation mediated by a clean rhodium surface during decomposition of both hydrazine and ammonia. The diimide formation has been detected over the 180–500 K temperature range as a gas-phase product resulting from hydrazine and ammonia decomposition on a Rh surface.

The experiments were performed in a UHV system equipped with Auger electron spectroscopy (AES), low-energy electron diffraction (LEED), and a multiplexed mass spectrometer for temperature-programmed reaction spectroscopy (TPRS). The base pressure after bakeout was 3.2×10^{-11} Torr. The rhodium foil was mounted on a manipulator, which allowed resistive heating

(1) Miller, C. E. *J. Chem. Educ.* **1965**, *42*, 254.
(2) Van Tamelen, E. E.; Dewey, R. S., Lease; M. F. and Pirkle, W. J. *J. Am. Chem. Soc.* **1961**, *83*, 4302.
(3) Alylward, F.; Sawistoska, M. *Chem. Ind. (London)* **1962**, 484.
(4) Fisher, H.; Gibian, H. *Justus Liebigs Ann. Chem.* **1941**, *548*, 183; **1942**, *550*, 208.
(5) Willis, C.; Back, R. A. *Can. J. Chem.* **1973**, *51*, 3605.
(6) Dows, D. A.; Pimentel, G. C.; Whittle, E. *J. Chem. Phys.* **1955**, *23*, 1606.
(7) Foner, S. F.; Hudson, B. F. *J. Chem. Phys.* **1958**, *28*, 719.
(8) Blau, E. J.; Hochheimer, B. F.; Ungen, H. J. *J. Chem. Phys.* **1961**, *34*, 1060.

0002-7863/91/1513-1577$02.50/0

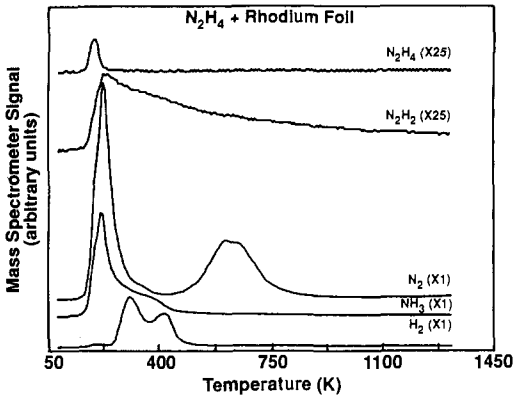

Figure 1. Thermal desorption spectrum illustrating the decomposition of adsorbed hydrazine on the rhodium surface. N_2H_2, NH_3, N_2, H_2 and N_2H_4 are the desorbing species observed.

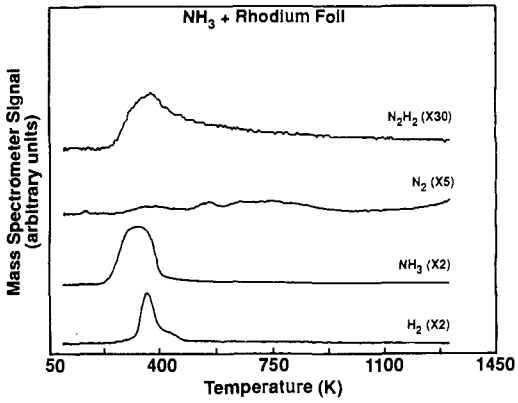

Figure 2. Thermal desorption spectrum illustrating the decomposition of adsorbed ammonia on the Rh surface. N_2H_2, NH_3, N_2, and H_2 are the desorbing species observed. The small peak at 550 K in the N_2 spectrum is the reuslt of a small amount of CO contamination. The total amount of CO was ~3% of the N_2 total.

to 1500 K and cooling to approximately 80 K. The temperature was monitored by a chromel–alumel thermocouple spot-welded to the back of the sample. The polycrystalline rhodium foil sample was cleaned by repeated heating to 800 K in 2×10^{-7} Torr oxygen and by argon ion bombardment. The TPRS data were recorded with a linear temperature ramp of 10 K s^{-1}. The sample was placed 2 mm from the mass spectrometer collimator and in direct line-of-sight to reduce background effects and eliminate contributions from support wires.

All gases were adsorbed at 80 K through a doser approximately 2.5 cm away from the surface. To minimize hydrazine decomposition inside the doser, the doser was preconditioned carefully by repeated, long-term exposure to hydrazine, and hydrazine was replaced frequently between the experiments. Hydrogen and nitrogen have been reported to be the gas-phase products of catalyzed hydrazine decomposition on most metals.[9] Thus, if hydrazine is predecomposed inside the doser, the rhodium surface will be dosed with a mixture of molecular hydrogen and nitrogen gases. Molecular nitrogen gas does not adsorb on the Rh surface at 80 K.[9] Therefore, the gas-phase products of hydrazine decomposition observed following exposure to predissociated hydrazine would be dominated by hydrogen. The data in Figure 1 clearly indicate that both gas-phase nitrogen and hydrogen are desorbed from a hydrazine-dosed surface. This result suggests that hydrazine is not predecomposed inside the doser and the rhodium surface has been dosed with molecular hydrazine during these experiments.

Typical desorption spectra generated following adsorption of N_2H_4 and NH_3 at 80 K are shown in Figures 1 and 2, respectively. For coverages of less than a monolayer, adsorbed hydrazine and

(9) Prasad, J.; Gland, J. L.; Slaughter, E.; Rufael, T. *Langmuir*, in press.

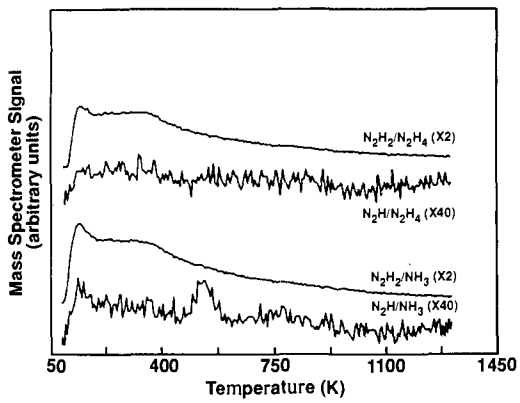

Figure 3. Thermal desorption spectra illustrating the desorption of N_2H_2 (30 amu) and a single-dehydrogenation fragmentation product (29 amu) of the parent N_2H_2 (30 amu). The peak at 550 K in N_2H/NH_3 is caused by the natural abundance of $^{13}C^{16}O$ in a minor CO contaminant. The interpreted value for the 29-amu peak at 550 K is ~1.3% of the 28-amu peak resulting from CO desorption. This is consistent with a ^{13}C natural abundance of ~1.1%.

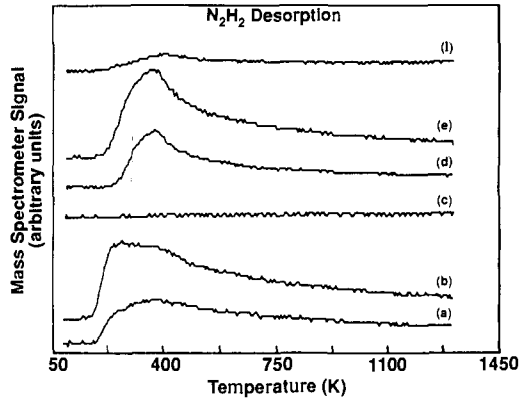

Figure 4. Thermal desorption of N_2H_2 following adsorption of (a) N_2H_4 only, (b) H_2 coadsorbed with N_2H_4, (c) O_2 coadsorbed with N_2H_4, (d) NH_3 only, (e) H_2 coadsorbed with NH_3, and (f) O_2 coadsorbed with NH_3.

ammonia both decompose on the Rh surface during a TPRS cycle giving N_2H_2, H_2, NH_3, and N_2. The kinetics of individual product formation will be discussed in detail elsewhere for N_2H_4 decomposition[9] and NH_3 oxidation.[10]

It has been reported that adsorbed imide (NH) is a stable intermediate during hydrazine and ammonia decomposition on Ni, Rh, Ir, W, and Mo surfaces.[11-15] This suggests a mechanism in which hydrazine and ammonia dissociatively adsorb on Rh dehydrogenating rapidly to form NH(ad), nitrogen atoms, and hydrogen atoms. We propose here that a portion of the NH(ad) recombines to form diimide, which desorbs from the Rh surface.

In previous studies, diimide formation was identified by measuring isotopic distribution (N_2H_2, N_2HD, N_2D_2) by use of mass spectrometry.[7] In our studies, diimide formation has been identified on the basis of the parent ion (30 amu) and a single-dehydrogenation fragmentation product (29 amu) that is ~6% of the parent. As shown in Figure 3, the temperature profile for mass 29 clearly follows that of mass 30, indicating that it is the fragmentation of the parent (30 amu). The yield and temperature profiles of masses 30 and 29 are independent from both the reactants and products, indicating a distant species is formed. Further evidence is discussed in the following paragraph, which

(10) Prasad, J.; Gland, J. L., submitted for publication in *Surf. Sci.*
(11) Gland, J. L.; Fisher, G. B.; Mitchell, G. E. *Chem. Phys. Lett.* **1985**, *119*, 89.
(12) Daniel, W. M.; White, J. M. *Surf. Sci.* **1986**, *171*, 289.
(13) Wood, B. J.; Wise, H. *J. Catal.* **1975**, *39*, 471.
(14) Cosser, R. C.; Tompkins, F. C. *Trans. Faraday Soc.* **1971**, *67*, 527.
(15) Contaminard, R. C. A.; Tompkins, F. C. *Trans. Faraday Soc.* **1971**, *67*, 545.

clearly indicates that a separate product is being formed.

Diimide formation has been confirmed chemically by observing the yield in the presence of coadsorbed hydrogen and coadsorbed oxygen with both hydrazine and ammonia on the Rh surface (Figure 4). In the presence of coadsorbed hydrogen, the yield of diimide increased substantially for both N_2H_4 and NH_3. In the presence of hydrogen, we propose that the concentration of NH(ad) may be higher, thus increasing the diimide yield. In the presence of coadsorbed oxygen, the yield of diimide decreases substantially. We propose that coadsorbed oxygen decreases the surface NH(ad) concentration, thus decreasing the yield of diimide formation.

In summary, diimide formation has been observed as a gas-phase product during hydrazine and ammonia decomposition on a clean Rh surface. Mass spectroscopy has been used to identify diimide. Diimide formation has been chemically confirmed since diimide yield increases substantially by coadsorption of hydrogen and decreases substantially by coadsorption of oxygen. Our results suggest that NH may be a stable surface intermediate during hydrazine and ammonia decomposition on Rh surface.

Strong Lewis Acids Derived from Molybdenum and Tungsten Nitrosyls Containing the Tri-2-pyridylmethane Ligand. Dynamic NMR Studies of Their Adducts with Aldehydes, Ketones, and Esters

J. W. Faller* and Yinong Ma

Contribution from the Department of Chemistry, Yale University, New Haven, Connecticut 06511.
Received June 27, 1990

Abstract: The doubly charged Lewis acid percursors $[HC(py)_3M(NO)_2(CO)](SbF_6)_2$ (M = Mo, W; $HC(py)_3$ = tri-2-pyridylmethane) are conveniently synthesized by reaction of $HC(py)_3M(CO)_3$ and 2 equiv of $NOSbF_6$. Facile loss of CO from the precursors generates the $[HC(py)_3M(NO)_2](SbF_6)_2$ Lewis acids. The Lewis acidity of the tungsten complex is greater than that of the molybdenum complex. With the ^1H NMR chemical shifts of bound crotonaldehyde as a qualitative assessment of relative acidity, the acidity of the tungsten species is comparable to that of BF_3 and $AlCl_3$, while that of the molybdenum species is similar to that of $TiCl_4$. Analysis of the NMR spectra of the Lewis acid–organic carbonyl base adducts, which include the adducts of aldehydes, ketones, and esters, showed that η^1-M(O=C) interactions dominate the chemistry. The barriers of rotation about the aldehyde C_1–C_2 bonds in the *p*-anisaldehyde adducts of the molybdenum and tungsten species were measured to be 12.8 and 13.7 kcal/mol, respectively, which are significantly higher than that for the free *p*-anisaldehyde. The exchange behavior between the *E* and *Z* isomers of the acetate adducts could be observed on the NMR time scale. The *E* to *Z* interconversion barriers of 12.2 ± 0.1 and 12.3 ± 0.1 kcal/mol for the methyl acetate and ethyl acetate complexes, respectively, were calculated from the results of variable-temperature proton NMR experiments. The free energy differences between the *E* and *Z* conformers of the methyl acetate and ethyl acetate adducts are 1.27 ± 0.01 and 0.96 ± 0.01 kcal/mol at 229 K, respectively.

Introduction

The complexation of organic carbonyl compounds with transition-metal complex Lewis acids can have a dramatic effect on the rates and selectivities of reactions at carbonyl centers, owing to the steric bulk and chirality of the ligands as well as to the electronic character of the metal centers.[1,2] An understanding of the structural and conformational aspects of the metal Lewis acid–carbonyl compound complexes should provide insight into reaction mechanisms, particularly with regard to selectivity. In the last decade, a number of transition-metal Lewis acid adducts of ketones and aldehydes have been isolated.[2,3] With a view to studying the interaction of transition-metal Lewis acids with carbonyl compounds, the reactions of $[HC(py)_3M(CO)(NO)_2](SbF_6)_2$ (M = Mo, W) with representative aldehydes, ketones, and acetate esters have been examined. NMR spectroscopic studies of various adducts have been undertaken, and the structural characteristics and chemical properties of these will be discussed here. The reaction of nitrosyl salts with low-valent transition-metal complexes have been widely used as a route to nitrosyl[4,5] complexes of both molybdenum and tungsten. Reaction of (tri-2-pyridylmethane)tricarbonylmolybdenum and -tungsten with nitrosyl hexafluoroantimonate forms highly charged cationic species $[HC(py)_3M(NO)_2(CO)](SbF_6)_2$. The high effective positive charge on the metal atom labilizes the π-acceptor ligand CO. This labilizing effect makes the $[HC(py)_3M(NO)_2(CO)](SbF_6)_2$ compounds excellent precursors for the facile generation of $[HC(py)_3M(NO)_2]^{2+}$ Lewis acids.

Experimental Section

Solvents were dried with use of standard procedures, and all manipulations were performed with Schlenk techniques unless specified otherwise. Proton NMR spectra were recorded at 250 and 500 MHz with Bruker spectrometers, and chemical shifts are reported (ppm) downfield from tetramethylsilane, with the solvent resonances for calibration. Temperatures were calibrated with the empirical correlation developed by Van Geet.[6] Nitromethane-d_3 was stored over molecular sieves under

(1) Sato, S.; Matsuda, I.; Izumi, Y. *Tetrahedron Lett.* **1986**, *27*, 5517.
(2) η^2-Ketone and aldehyde complexes: (a) Fernández, J. M.; Emerson, K.; Larsen, R. H.; Gladysz, J. A. *J. Am. Chem. Soc.* **1986**, *108*, 8268 and references therein. (b) Harman, W. D.; Fairlie, D. P.; Taube, H. *J. Am. Chem. Soc.* **1986**, *108*, 8223 and references therein. (c) Countryman, R.; Penfold, B. R. *Chem. Commun.* **1971**, 1598. (d) Kropp, K.; Skibbe, V.; Erker, G.; Krüger, C. *J. Am. Chem. Soc.* **1983**, *105*, 3353. (e) Brunner, H.; Wachter, J.; Bernal, I.; Creswick, M. *Angew. Chem., Int. Ed. Engl.* **1979**, *18*, 861. (f) Kaiser, J.; Sieler, J.; Walther, D.; Dinjus, E.; Golic, L. *Acta Crystallogr.* **1982**, *B39*, 1584.
(3) η^1-Ketone and aldehyde complexes: (a) Silverthorn, W. E. *Chem. Commun.* **1971**, 1310. (b) Williams, W. E.; Lalor, F. J. *J. Chem. Soc., Dalton Trans.* **1973**, 1329. (c) Foxman, B. M.; Klemarczyk, R. T.; Liptrot, R. E.; Rosenblum, M. *J. Organomet. Chem.* **1980**, *187*, 253. (d) Schmidt, E. K. G.; Thiel, C. H. *J. Organomet. Chem.* **1981**, *209*, 373. (e) Boudjouk, P.; Woell, J. B.; Radonovich, L. J.; Eyring, M. W. *Organometallics* **1982**, *1*, 582. (f) Bennett, M. A.; Matheson, T. W.; Robertson, G. B.; Steffen, W. L.; Turney, T. W. *Chem. Commun.* **1979**, 32. (g) Huang, Y.-H.; Gladysz, J. A. *J. Chem. Educ.* **1988**, *65*, 298.
(4) (a) Green, M.; Taylor, S. H. *J. Chem. Soc., Dalton Trans.* **1972**, 2629. (b) Sen, A.; Thomas, R. *Organometallics* **1982**, *1*, 1251.
(5) Stewart, R. P., Jr.; Moore, G. T. *Inorg. Chem.* **1975**, *14*, 2699.
(6) Van Geet, A. L. *Anal. Chem.* **1970**, *42*, 679.

0002-7863/91/1513-1579$02.50/0